JOURNAL OF MATERIALS SCIENCE **38** (2003) 4055–4063

Dielectric properties of nanostructured nickel oxide

V. BIJU, M. A. KHADAR*
Department of Physics, University of Kerala, Thiruvananthapuram, Kerala 695 581, India
E-mail: makhadar@mail.com

Nanostructured NiO samples having different average particle sizes were prepared and the variations of the real and imaginary components of the complex dielectric function ε^* were studied as a function of the frequency of the applied signal and temperature. The dielectric relaxation mechanism is discussed considering nanostructured NiO as a carrier dominated dielectric with high density of hopping charge carriers. The observed ω^{n-1} dependence of the real and imaginary components of ε^* is discussed in the light of the 'Universal' model of dielectric response. The various contributions to the measured dielectric loss ε'' such as the steady state charge transport, delayed readjustment of screening charges and the Debye delays are discussed. It is shown that the temperature dependence of both the real and imaginary components of ε^* are in accordance with the models used for discussing the dielectric relaxation and loss mechanisms. The variation of ε' with average particle size seems to be rather complex depending on a number of parameters associated with the interfacial region which vary with the average particle size.

1. Introduction

The electrical properties of nanostructured materials, which in most cases precipitously differ from those of their single crystalline, coarse-grained polycrystalline and thin film counterparts is of great theoretical and technological importance. The high surface to volume ratio of the grains, enhanced contribution from the interfacial region, possibility of high defect density, band structure modification and quantum confinement of charge carriers are some of the major factors determining the electrical response of nanostructured materials [1–8].

NiO is classified as a Mott-Hubbard insulator, for which the collective electron treatment used by Bloch and Wilson fails to explain the very low value of the experimentally observed conductivity, which is of the order of 10^{-13} ohm^{-1} cm^{-1} at room temperature [9–16]. Conductivity of NiO may be increased by introduction of Ni^{2+} vacancies and or by doping with monovalent cations like Li^+ [9–16]. Studies of the complex dielectric constant ε^* of NiO single crystals, polycrystals and thin films have been reported [16–20]. In undoped NiO, electrical conduction is primarily due to the hopping of holes associated with the Ni^{2+} vacancies [9–16]. However, the contribution of these hopping charge carriers to polarization is not fully understood [9–20]. Further, studies of the complex dielectric constant of nanostructured NiO has not been reported so far. In our earlier studies, the dc and ac conductivities of nanostructred NiO was found to be enhanced by six to eight orders of magnitude over those of NiO single crystals [21–23]. The present paper reports the studies of the complex dielectric function of consolidated nanoparticles of NiO having different average particle sizes as a function of frequency of the applied signal and temperature.

2. Experimental

Nickel carbonate nanoparticles were prepared through arrested chemical precipitation method. NiO nanoparticles having different average particle sizes were obtained by the thermal decomposition of the carbonate precursor followed by air annealing. Details of sample preparation are reported elsewhere [21–23]. The average size of the particles were calculated from the line broadening of the X-ray diffraction peaks corrected for instrumental broadening using Scherrer's equation and are listed in Table I together with the sample codes assigned for convenience [24].

The nanoparticle samples were consolidated in the form of cylindrical pellets of 13 mm diameter and thickness about 1 mm by applying a uniaxial force of 4 tons for two minutes using a hydraulic press. Conducting silver epoxy was applied on both the faces of the pellets to serve as electrodes. The pellets were first air dried for 30 min and then heat treated at 90°C for 15 min in a hot air oven for electrode curing. Electrical measurements were carried out in an evacuated dielectric cell. Before taking measurements each pellet was subjected to a heat and cool run between 313 and 413 K in

*Author to whom all correspondence should be addressed.

TABLE I Details of nanostructured NiO samples

Sample code	Average particle size (nm)
N1	2–3
N2	4–5
N3	5–7
N4	12–13
N5	16–17

vacuum for removing any residual strain due to pelletisation. The complex impedance Z^* and the phase angle θ were measured at different signal frequencies ranging from 100 Hz to 3 MHz using a Hioki Model 3531 Z-Hi Tester. The measured parameters Z^* and θ were found to be independent of the magnitude of the input signal voltages ranging from 0.1 to 1 V. This implies that the observed dielectric response is not associated with the electrode-sample interface, which would have been very non-linear in this range of voltages [25–27]. Parallel equivalent circuit model was chosen for analyzing the data due to the high dielectric loss exhibited by the samples [26]. The real and imaginary components of the complex dielectric function ε^* was calculated from the measured data knowing the dimensions of the pellets [25, 26].

3. Results

Figs 1a, b, 2a and b show the frequency dependence of the real part ε' and the imaginary part ε'' of the complex dielectric constant of the samples at three different temperatures in the frequency range 100 Hz–3 MHz. The values of ε' of all the samples show large variation as the frequency of the applied signal is varied (Fig. 1a and b). The numerical value of ε' at low frequencies for samples N1, N2 and N3 is of the order of 10^4 to 10^3 while it is of the order of 10^3 to 10^2 for samples N4 and N5. The frequency dispersion of all the samples exhibit two distinct regions of frequency response. The two distinct regions with markedly different slopes are more clearly notable in the frequency dispersion of samples N1 and N2, having smaller average particle sizes than in the case of samples N3, N4 and N5 with relatively larger average particle sizes (Fig. 1a and b). Also for none of the samples the value of ε' reach a frequency independent high frequency limiting value (ε'_∞) even at 3 MHz, the highest frequency in the present study. This is in sharp contrast with the case of both single crystalline and coarse-grained polycrystalline NiO for which ε' has a limiting value of $\approx$11.9 at frequencies $\geq\sim$10 kHz [17–19]. From Fig. 2a and b it is clear that the dielectric loss ε'' of all the samples have large values $\sim 10^4$ to 10^6 at low frequencies, which falls off as the frequency of the applied signal is increased. The frequency response of ε'' does not show any well-defined loss peak for any of the samples in the region of observation. However, a careful analysis of the frequency response of ε'' for sample N2 show possible presence of a loss peak centered at $\sim$50 kHz. It may be noted from Figs 1 and 2 that in the low frequency region, the imaginary component ε'' shows a comparatively steeper rise with decrease in the applied signal frequency than the real component ε'.

The temperature dependent variation of ε' for the samples at three different frequencies is shown in Fig. 3 and that of ε'' is shown in Fig. 4. Both ε' and ε'' increase with increase in temperature over the entire

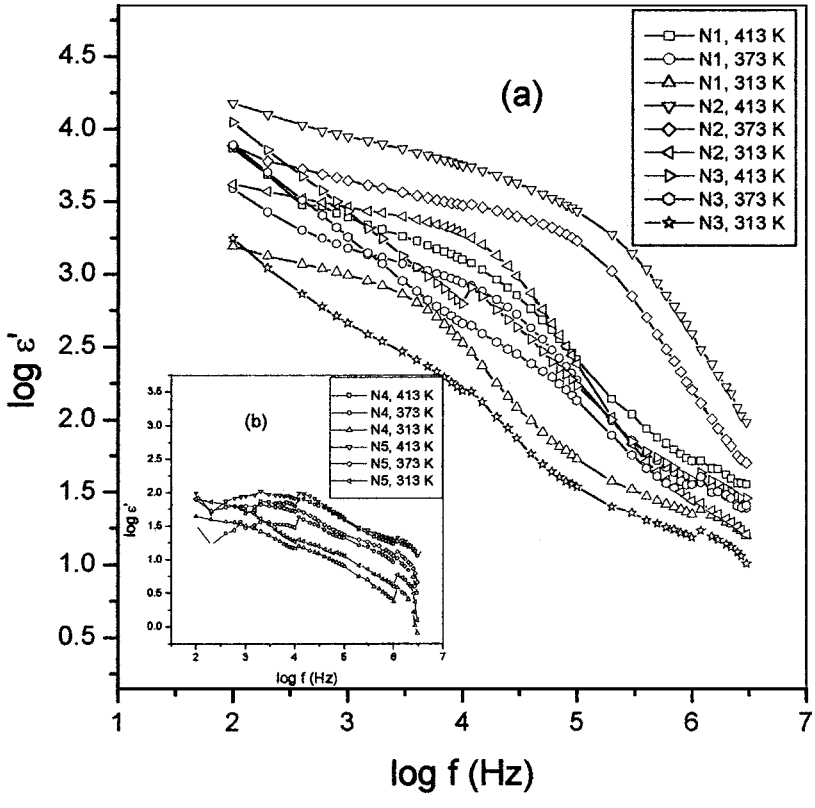

Figure 1 Variation of ε' with frequency for samples: (a) N1, N2, N3 and (b) N4 and N5.

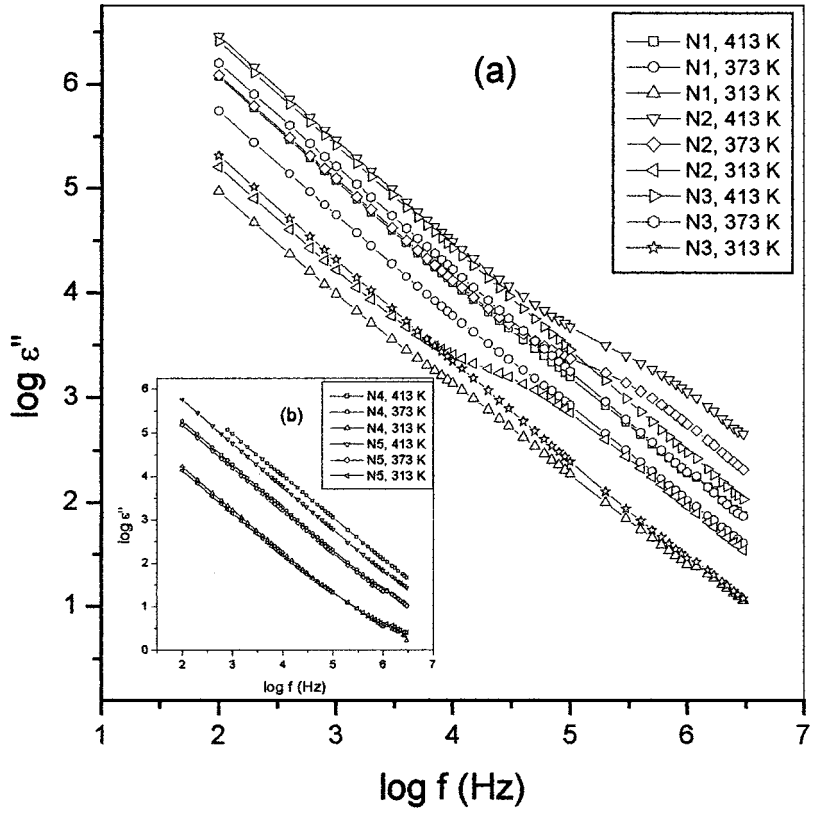

Figure 2 Variation of ε'' with frequency for samples: (a) N1, N2, N3 and (b) N4 and N5.

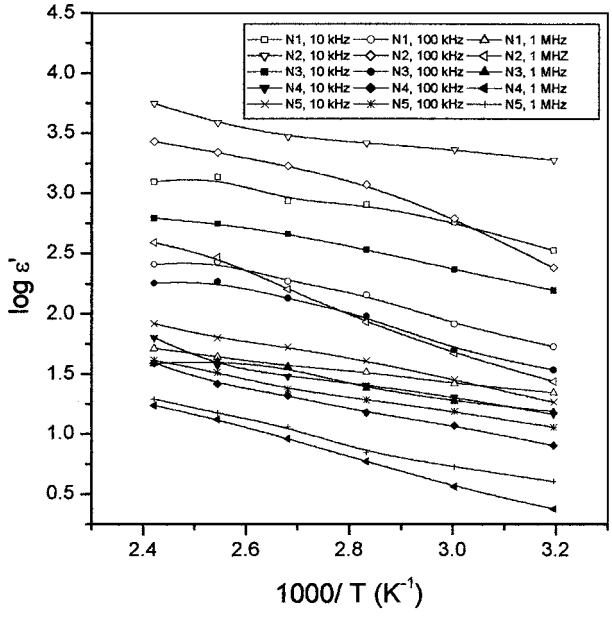

Figure 3 Variation of ε' with temperature for samples N1, N2, N3, N4 and N5.

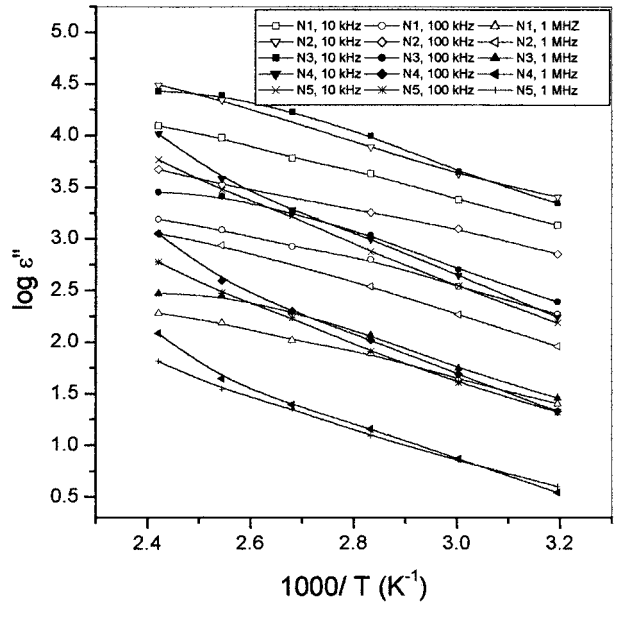

Figure 4 Variation of ε'' with temperature for samples N1, N2, N3, N4 and N5.

frequency range with well defined activation energies (Figs 3 and 4).

4. Discussion

It has been reported that nanoparticles of semiconductors like ZnS, ZnO and superionic conductors such as $AgHgI_4$ show an increase in the values of both ε' and ε'' in comparison with their single crystalline counterparts [6–8]. Size effects on the dielectric constant, ferroelectricity and domain structure of nanocrystalline $PbTiO_3$ and $BaTiO_3$ have also been reported [3, 4]. In our earlier studies, we had observed that both dc and ac conductivities of consolidated nanoparticles of NiO was enhanced by six to eight orders over that of undoped NiO single crystals [21–23]. This was attributed to the high concentration of Ni^{2+} vacancies associated with the grain boundaries of NiO nanoparticles, which was estimated to be $\sim 10^{14}$ to 10^{16} cm^{-3} [21–23].

In undoped NiO, each Ni^{2+} vacancy in the lattice causes the transformation of two adjacent Ni^{2+} ions into

Ni^{3+} ions for acquiring charge neutrality and this transformation induces a local lattice distortion [9, 10]. The lowest possible energy state for this system consisting of one Ni^{2+} vacancy and two adjacent Ni^{3+} ions is that of a quadrupole complex [10]. In presence of an electric field, the two holes associated with the quadrupole complex can contribute to conduction by hopping [9–11]. The energy barrier to be overcome by the holes for hopping between lattice sites will depend on a number of factors. At a single lattice site, a short range localization energy will arise because of the random fluctuations in the site separation or atomic configuration or polaron effects. In addition, associated with each Ni^{2+} vacancy, there exists a long range potential well that affects the localization energy within a few lattice spacings [11, 28]. When an electric field is applied, two types of hopping processes can occur in NiO—the long range inter-well hopping which involves the hopping of holes between sites located in adjacent defect potential wells and the short range intra-well hopping of holes between sites located within one defect potential well. The inter-well hopping corresponds to steady state transport of charge carriers between the electrodes, i.e., the dc contribution to the total ac conductivity, while the intra-well hopping constitutes the pure ac conduction [11, 28]. The frequency and temperature dependence of the inter-well and intra-well hopping mechanisms are markedly different from one another [11, 28]. In the following discussion an analysis of the respective contributions of the inter-well and intra-well hopping to ε' and ε'' of nanostructured NiO is presented.

The sample pellets used in the present study were dry pressed and were not sintered and hence some porosity may be present in them. Since, the samples were prepared by thermal decomposition of the carbonate precursor followed by annealing, the possibility of presence of pore fluids and adsorbed water is exceedingly small. The only possible moisture content should be that from air occluded during pelletisation. However, all the pellets were subjected to heat and cool runs between 313 and 413 K in vacuum before the electrical measurements and hence the moisture content and occluded air, if any, might almost completely be removed. Nan *et al.*, had reported that the contribution of pores to the ac electrical data will manifest as a low frequency semicircular arc in the complex $Z' - Z''$ plot with equivalent circuit parameters having the same temperature dependence as those for the high frequency semicircular arc representing the grain interior ac response [2]. This in turn means that the relaxation times corresponding to the electrical processes associated with the grain interior and porosity will have the same temperature dependence. In our earlier impedance spectroscopic study of nanostructured NiO samples, we had observed that the $Z' - Z''$ plots consist of two well resolved semicircular arcs—one at high frequencies and the other at low frequencies—with relaxation times exhibiting markedly different temperature dependences indicating that the low frequency semicircular arc is not associated with the pores [21]. We concluded that the contribution of pores to ac conductivity data of the nanostructured NiO samples, if at all any, is minimal.

4.1. Dielectric relaxation mechanism

As stated earlier, the nanostructured NiO samples in the present study have a high density of Ni^{2+} vacancies (10^{14} to 10^{16} cm^{-3}) each of which can contribute two holes for charge transport [21–23]. Hence, nanostructured NiO can be picturised as a dielectric material with very high concentration of hopping charge carriers—viz. carrier dominated dielectric. A wide range of carrier dominated dielectrics have been reported to have very large values of both ε' and ε'' at low frequencies and strong frequency dispersion similar to our observation (Figs 1 and 2) [27, 29–33]. The large values of ε' at low frequencies in dielectrics with high density of hopping charge carriers may be understood on the basis of the definition of polarization as the dipole moment per unit volume

$$P = \sum_{\propto} x_\alpha q_\alpha \tag{1}$$

where α takes into account all charged particles in the system, q represents the respective charges and x the displacement under an applied electric field [27]. It is known that a 'typical' molecular displacement of an electron cloud with respect to the nucleus or two neighboring ions with respect to one another in an applied field of the order of 10^6 Vm^{-1} may be of the order of 10^{-4} nm [27]. In dielectrics with hopping carriers, a few inter atomic jumps involving several atomic displacements typically of the order of a few Å to a few nm result in a considerable increase of polarization and hence of apparent ε' [27]. Further, the high density of hopping charge carriers causing high dc conductivity accounts for the high dielectric loss at low frequencies.

In NiO samples, when an ac field is applied both inter-well and intra-well hopping mechanisms do have a finite probability of occurrence, their relative probabilities being dependent on the energy of the charge carriers, frequency of the applied signal and concentration, mean site separation, depth and extent of percolation of the potential wells associated with Ni^{2+} vacancies [11, 28]. According to the Correlated Barrier Hopping (CBH) model, the inter-well hopping is the predominant process at low frequencies [11, 28]. In general, inter-well hopping which corresponds to the steady state transport of charge carriers between the electrodes does not contribute to polarization [11, 28]. However, in nanostructured NiO, owing to the high density of Ni^{2+} vacancies concentrated at the highly disordered grain boundaries, there will be a reasonable extent of percolation of adjacent defect potential wells. According to earlier reports, such an overlapping of defect potential wells will manifest as a decrease in the activation energy for dc conduction [11, 28]. We had observed that the activation energy for dc conductivity of nanostructred NiO is about 0.2 eV less than that for corresponding single crystals in agreement with the above report and indicating the probability of overlapping of defect potential wells [22]. This probability for overlapping of potential wells leads to the argument that at least a few holes executing inter-well hopping do reverse the direction of motion when the electric field direction reverses

and thus inter-well hopping may also contribute to dielectric relaxation at low frequencies. This reasoning is consistent with the high density of Ni^{2+} vacancies is nanostructured NiO. The average hopping distance for inter-well hopping is the mean site separation of the Ni^{2+} vacancies, which is roughly estimated to be of the order of a few nanometers from the Ni^{2+} vacancy concentration obtained from the conductivity studies [21–23]. This according to Equation 1 corresponds to very high value of polarization and hence of apparent ε' of the order of 10^2 to 10^4 [11, 21–23, 28]. Thus the large values of ε' observed for all the NiO nanoparticle samples in the present study at frequencies less than or equal to 10^3 Hz may be attributed to the contribution from a portion of charge carriers undergoing inter-well hopping which reverses the direction of motion on reversal of the field.

As the signal frequency is increased to higher values, the probability of occurrence of intra-well hopping becomes large since the charge carriers do not get enough time for long range hopping before field reversal [32]. The average hopping distance for intra-well hopping is one lattice spacing, ≈4.2 Å for NiO, while it is of the order of a few nanometers for inter-well hopping as already mentioned [11, 28]. Thus according to Equation 1 polarization decreases as the signal frequency is increased. At still higher frequencies, i.e., in the MHz range, the charge carriers would barely have started to move before the field alters its direction and ε' falls rapidly to very smaller values. The observation that the high frequency values of ε' for nanostructured NiO falls below ε'_{∞} for single crystalline NiO is possibly due to the high concentration of holes associated with the grain boundaries of nanostructured samples and the fact that the grain interior of nanocrystalline samples is generally devoid of defects and inhomogeneties [34, 35]. As discussed earlier, at high frequencies, >1 MHz, the hopping charge carriers, associated with the Ni^{2+} vacancies mainly concentrated at the grain boundaries contribute very little to ε'. Also the lattice contribution to ε' from the grain interior will be very less since barely any charge carriers will be present at the grain interior. The above argument that the grain interior of nanostructured NiO is practically devoid of hopping charge carriers is well complemented by reported studies on the electrical nature of NiO grain boundaries and molecular dynamics studies [36–41]. The studies of the electrical nature of NiO surfaces conclude that the Ni^{2+} vacanices and hence associated charge carriers are concentrated near the grain boundaries leading to high surface conduction while the molecular dynamics studies through quantitative estimations establishes that the accumulation of Ni^{2+} vacancies near the surface region corresponds to an energetically more favorable condition [36–41].

The above discussion may be extended for explaining the observed high values of ε'' at low frequencies as well as its stronger frequency dependence in the low frequencey region in comparison with that of ε'. As discussed earlier, in the low frequency region inter-well hopping which corresponds to the steady state conduction is the predominant process. This explains the high dielectric loss in the low frequency region [27, 29, 30]. Also, according to the above discussion, due to the overlapping of the defect potential wells only a small fraction of the total number of holes executing long-range hopping reverses direction on field reversal and thus contributing to polarization, while the majority of the holes contribute to energy loss due to steady state charge transport between the electrodes. This explains why the increase of ε'' with decrease in frequency is steeper in comparison with that of ε' in the low frequency region.

4.2. Frequency dispersion

In this section the observed frequency dispersion of both the real and imaginary parts of ε^* will be analyzed on the basis of the 'Universal' dielectric response model of solids, emphasizing the physical basis for such a response to occur in dielectrics with high concentration of hopping carriers such as nanostructured NiO. It may be noted that the frequency dispersion of ε'' presented in Fig. 2, which show no loss peaks, includes the contribution due to the steady state transport of charge carriers between electrodes (dc conduction), since no dc correction has been applied. According to the earlier studies on carrier dominated dielectrics with high concentration of charge carriers, the dc contribution will cause a nearly $1/\omega$ dependence of ε'' at lower frequencies and loss peak associated with any possible relaxation mechanism will be submerged in the dominant dc contribution [27, 29, 30]. Further, the steady state transport of charge carriers will not generally contribute to polarization and hence to ε' since the dc conduction does not change the center of gravity of charge distribution [27, 29]. This makes ε' a comparatively weaker function of frequency in the low frequency region. The above discussion together with the analysis of Figs 1 and 2 suggest that the frequency response of ε'' of nanostructured NiO samples is dominated by dc contribution and dc correction should be done for detailed analysis.

In order to find the dc contribution (σ_{dc}) to the measured ac conduction, a two step curve fitting procedure devised by Jonscher was employed [27, 30]. In the first step nonlinear least square fitting was done on $Y'' - \omega$ plots using the equation $Y'' = A_n(\omega)^n$ where $Y'' = \mathrm{Sin}\ \theta/|Z^*|$ is the imaginary part of the complex admittance function, A_n is a constant, $\omega = 2\pi f$ is the angular frequency of the applied ac signal and n (with $0 < n < 1$) is a measure of the deviation of the sample from ideal Debye behavior [27, 30]. In the second step nonlinear least square fitting was done on $Y' - \omega$ plots using the equation $Y' = [G_v + \omega^n A_n \mathrm{Cot}\,(n\pi/2)]$ using the values of A_n and n obtained from the first curve fitting procedure. Here $Y' = \mathrm{Cos}\theta/|Z^*|$ is the real part of the complex admittance function (measured ac conductance) and G_v is the pure dc contribution to Y'. From G_v values, σ_{dc} values were calculated knowing the dimensions of the pellets for all the samples. The results of curve fitting procedure for the sample N2 at 333 K are shown in Fig. 5a and b.

The dispersion of ε'' after dc correction for sample N2 at different temperatures are shown in Fig. 6a and those for different samples at two different temperatures

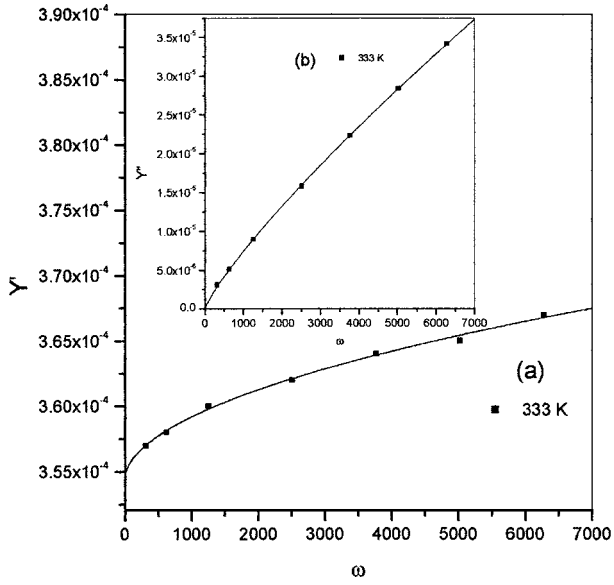

Figure 5 Results of curve fitting procedure for the sample N2 at 333 K: (a) $Y' - \omega$ plot and (b) $Y'' - \omega$ plot.

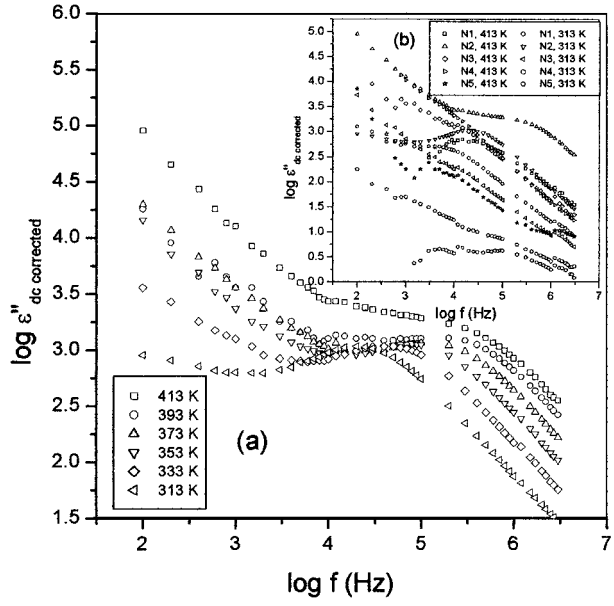

Figure 6 Variation of dc corrected ε'' with frequency: (a) for sample N2 at different temperatures and (b) for different samples at 413 K and 313 K.

are shown in Fig. 6b. Fig. 6a and b show that after dc correction the broad loss peaks are well resolved for samples N1 and N2 of smaller particle sizes while those for samples N3, N4 and N5 of larger particle sizes are not so resolved. The shifting of the loss peak maxima shifts to higher frequencies with increase in temperature as seen from Fig. 6a implies that the relaxation time constant $\tau = 1/\omega_{\mathrm{m}}$, ω_{m} being the frequency of the applied signal at the peak maxima, corresponds to a thermally activated process and that it has a negative temperature coefficient.

Analysis of Figs 1, 2 and 6 reveal that the frequency dispersion of the real and imaginary components of ε^* deviate from ideal Debye response [42–50]. Rather, both ε' and ε'' data exhibit $\omega^{\mathrm{n}-1}$ dependence with $n < 1$ in accordance with the "Universal model" of dielectric response of solids put forward by Jonscher [42–50]. The usual practice of accounting for such non-Debye behavior is to introduce an arbitrary distribution function $g(\tau)$ for the time constant in the Debye equation, which corresponds to a superposition of Debye-like relaxation times [42–46, 49]. The concept of $g(\tau)$ is superficially very plausible especially for disordered systems such as nanostructured NiO samples in the present study, but has physically little meaning [42–46, 49]. However, the 'Universal' model does not relay on any arbitrary function for explaining the non-Debye behavior and envisages that rather than being the result of a superposition of Debye-like relaxation times the $\omega^{\mathrm{n}-1}$ dependence is the manifestation of a universal mechanism for which the ratio of the energy lost per cycle to the energy gained per cycle is independent of frequency [42–50]. The $\omega^{\mathrm{n}-1}$ dependence exhibited by a wide range of solid dielectrics is in fact due to the many body interactions in these materials in presence of an ac electric field [44–46, 49, 50]. In fact, the Debye theory has nothing in it for including the possible many body interactions between dipoles or hopping carriers and hence fails to explain the frequency response of materials for which there exist strong interactions between dipoles or hopping carriers such as nanostructured NiO. The mechanism of "screened hoping" of charge carriers, which is the kind of many body interaction most probable in nanostructured NiO leading to the observed non-Debye behavior is discussed below.

For materials with high density of hopping carriers, as in the present case of NiO nanoparticles, the many body interpretation of the universal response is based on a semi quantitative 'screened hopping model' [27, 29, 43–45]. The screened hopping model is applicable to systems in which discontinuous hopping of charge carriers occurs between localized positions in presence of a 'screening charge' adjusting slowly to the rapid hopping [43]. Further, the model introduces a parameter 'p' which characterizes the strength of screening with: heavy screening (strong many body interactions) corresponding to $p \to 0$ while the absence of screening (absence of many body interactions) corresponding to $p = 1$ [29, 43]. Also it was shown that the parameter 'p' and the exponent 'n' are related by $\cot(n\pi/2) = (1-p)/p$. Thus $n \to 1$ when $p \to 1$ and $n \to 0$ as $p \to 0$ [29, 43]. Hence the numerical value of the exponent 'n' may be considered to be a measure of the extent of many body interactions in the dielectric material. In nanostructured NiO samples, there exist a large number of holes associated with Ni^{2+} vacancies, which execute discontinuous hopping between lattice sites in presence of an ac field [21–23]. Each hole localized at a lattice site imposes a coulomb like potential on the surrounding medium and this tends to repel positive charges and attract electrons that may be present in the neighborhood, thus bringing about a partial screening of the holes. In NiO, which is a dielectric with localized charges, the screening would not be complete since the localized charges are not quite free to assume the exact local arrangement demanded by the local value of the potential [10, 37, 43]. With every single hopping of the holes, these partial screening charges will be

readjusting and this causes a reduction in the effective polarization from qr_{ij} to pqr_{ij} where $0 < p < 1$ is a measure of the extent of screening as already mentioned. For NiO, 'q' is $+e$ and r_{ij} is the hopping distance involved. The reduction in polarization corresponds to a reduction in potential energy of the system and the energy loss involved is dissipated through phonon system [43]. This is the major contribution to the dc corrected ε'' which show ω^{n-1} dependence.

A detailed analysis of the frequency dispersions of ε', measured ε'' and dc corrected ε'' reveals that all the three quantities show ω^{n-1} dependence with $0 < n < 1$. It was found that the measured ε'' of all the five samples have very small 'n' values ranging from 0.03 to 0.2. This is due to the onset of dc conduction as explained in the previous section [27, 29, 30]. Further, ε' and dc corrected ε'' data of the samples N1 and N2 (samples having smaller average particle sizes) show two well differentiated regions- low frequency and high frequency- with different 'n' values. For both N1 and N2 the ε' dispersion has 'n' values ranging from 0.6 to 0.85 in the low frequency region while at higher frequencies 'n' lies between 0.2 and 0.6. As mentioned earlier, the numerical value of 'n' is a measure of the degree of screening. Thus for samples N1 and N2, at higher frequencies, the holes undergo short-range hopping and this leads to only a slight readjustment of screening charges corresponding to smaller values of 'n'. However, at lower frequencies, the long range hopping demands a greater extent of readjustment of screening charges. Since the screening charges in NiO (i.e., electrons) are well localized, this leads to a decrease in screening and hence increase in 'n' [9–15].

It was found that the frequency dispersion of ε' of each of the samples N3, N4 and N5 has a single slope throughout the entire range of frequencies. For all the three samples the exponent 'n' for ε' dispersion lies between 0.4 and 0.6. The absence of a marked difference between the low frequency and high frequency 'n' values for ε' of the samples N3, N4 and N5 is attributable to the relatively larger average particle sizes of these samples in comparison with N1 and N2. It has been reported that the disordered nature of the grain boundaries, mechanical micro stress, surface energy and any surface domain depolarization phenomena will affect the dielectric response of nanostructures [3, 4]. From the presently available data of nanostructured NiO samples, we can only conclude that the difference in the low and high frequency dispersions of ε' is not evident for samples N3, N4 and N5 due to their lower interfacial volume fraction in comparison with that for N1 and N2.

According to the energy criterion leading to ω^{n-1} dependence, both ε' and dc corrected ε'' should have exactly the same 'n' value [42–50]. But in the present case slightly smaller values of 'n' for dc corrected ε'' than those for ε' were observed. This is only as expected because in the above discussion we have considered the dielectric loss due to the delayed readjustment of screening charges only. This fraction of the total loss is over and above that due to any natural Debye delay in the response of hopping charges which give rise to a loss given by Debye equation, since such Debye losses are not excluded from ε'' on carrying out dc correction [43]. Since Debye delays do not contribute to the polarization (ε') but contribute to dielectric loss (ε''), the dc corrected ε'' is more strongly dependent on frequency (i.e., smaller 'n' values) than ε'.

4.3. Temperature dependence

Fig. 3 clearly shows that the real component ε' increase with increase in temperature over the entire frequency range for all the samples with well defined activation energies which points to the fact that the polarization is due to some thermally activated mechanisms such as charge carrier transport rather than due to permanent dipoles [30]. This is in agreement with our discussion on the dielectric relaxation mechanism and observed frequency response based on hopping of holes associated with Ni^{2+} vacancies. Activation energies for ε' of nanostructured NiO samples was found to lie between 0.1 and 0.3 eV in the present study. Earlier studies on single crystalline NiO have also reported an increase in the value of ε' with increase in temperature with an activation energy of $\approx$0.2 eV above 313 K [17]. The above agreement of the values of the activation energies of ε' leads to the conclusion that the mechanism of polarization is similar in both single crystalline and nanostructured NiO, while the nanostructured samples differ enormously from their bulk counterparts in the number of charge carriers involved, the average hopping distances and the number, mean site separation, depth and extend of overlap of the defect potential wells. Also, it was noted that the activation energies for the measured ε'' (without dc correction) which varies between 0.2 and 0.4 (Fig. 4) was very much close to the activation energies for total ac conductivity $\sigma_m = \sigma_{dc} + \sigma_{ac}$ obtained in our earlier studies [23]. Further, the activation energies for the dc corrected ε'' which lies between 0.1 and 0.3 is in agreement with that for the pure ac conductivity σ_{ac} [23]. These results complement our discussion on the contribution of pure dc conduction and delayed readjustment of screening charges to the measured ε''.

4.4. Dependence on particle size

The variation of ε' with particle size follows a pattern similar to that for the dielectric relaxation intensity as evident from Fig. 7. A similar increase and then fall in the value of ε' with increase in particle size was reported for nanostructured $BaTiO_3$ and $PbTiO_3$ samples where the observations were explained as the resultant of a number of factors such as the disordered structure of the surface region (amorphousness), surface energy, micro mechanical stress, surface domain depolarization phenomena, domain wall effects, etc. [3, 4]. In our earlier studies, we have observed a more or less similar dependence of dc and ac conductivities of nanostructured NiO on average particle size and have explained the results semi-quantitatively taking into consideration

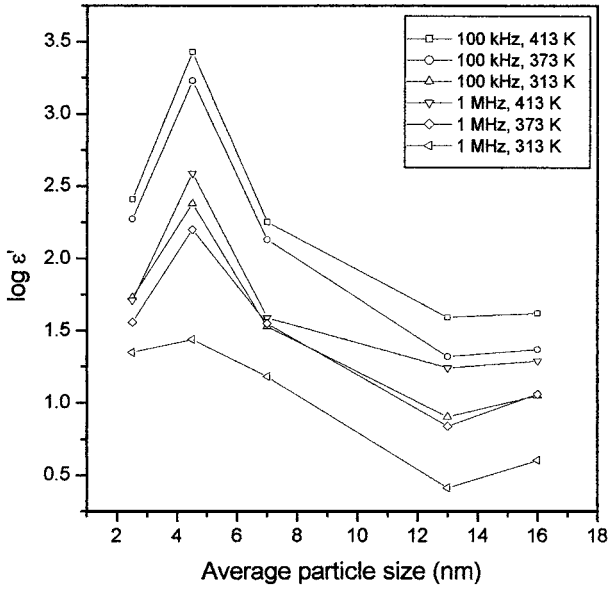

Figure 7 Variation of ε' with average particle size.

the special features of the structure of the interfacial region of nanostructures [22, 23]. It was pointed out that at particle sizes less than 10 nm, triple junctions (intersection lines of three or more grains which are analogous to dislocations and hence correspond to maxima of a potential barrier) constitute a considerable volume fraction of the total interface and affect the charge carrier transport [22, 23]. From the presently available data it is not possible to reach a quantitative explanation for the observed size dependence of ε' and one can only conclude that the observed results are manifestations of the interplay of a number of factors such as the structure of the interfacial region, volume fractions of grain boundaries and triple junctions, surface energy, micro stress, high surface conductance, Ni^{2+} vacancy distribution, etc., which affect the polarization mechanism.

5. Conclusion

NiO nanoparticle samples having different average particle sizes were prepared and the variations of the real and imaginary components of the complex dielectric function ε^* were studied as a function of frequency of the applied signal and temperature. The dielectric relaxation mechanism is discussed considering nanostructured NiO as a carrier dominated dielectric with high density of hopping charges. The observed ω^{n-1} dependence of the real and imaginary components of ε^* is discussed in the light of the 'Universal' model of dielectric response. The size dependent variation of ε' seems to be rather complex depending on a number of parameters associated with the interfacial region which varies with particle size.

Acknowledgement

One of the authors, V. Biju acknowledges the financial assistance provided by Council of Scientific and Industrial Research (CSIR), Government of India in the form of Senior Research Fellowship.

References

1. P. MARQUARDT, *Phys. Lett.* A **123**(7) (1987) 365.
2. CE-WEN NAN, A. TSCHOPE, S. HOLTEN, H. KLIEM and R. BIRRINGER, *J. Appl. Phys.* **85**(11) (1999) 7735.
3. B. JIANG, J. L. PENG, L. A. BURSIL and W. L. ZHONG, *ibid.* **87**(7) (2000) 3462.
4. A. S. SHAIK, R. W. VEST and M. G. VEST, IEEE. *Trans. Ultrason. Ferroelectr. Freq. Control.* **36** (1989) 407.
5. M. ABDUL KHADAR and B. THOMAS, *Nanostruct. Mater.* **10**(4) (1998) 593.
6. B. THOMAS and M. ABDUL KHADAR, *Pramana. J. Phys.* **45** (1995) 431.
7. JOSHY JOSE and M. ABDUL KHADAR, *Nanostruct. Mater.* **11**(8) (1999) 1091.
8. S. S. N. POTTY and M. ABDUL KHADAR, *Bull. Mater. Sci.* **23** (2000) 361.
9. F. J. MORIN, *Phys. Rev.* B **93**(6) (1954) 1199.
10. DAVID ADLER and JULIUS FEINLEIB, *ibid.* **2**(8) (1979) 3112.
11. A. J. BOSMAN and H. J. VAN DAAL, *Adv. Phys.* **19**(77) (1970) 1.
12. P. PUSHPARAJAH and S. RADHAKRISHNA, *J. Mater. Sci.* **32** (1997) 3001.
13. A. J. BOSMAN and CRREVECOEUR, *Phys. Rev.* **144**(2) (1965) 763.
14. S. VAN HOUTEN, *J. Phys. Cem. Solids.* **17**(1/2) (1960) 7.
15. R. R. HEIKES and W. D. JOHNSTON, *J. Chem. Phys.* **26**(3) (1957) 582.
16. P. LUNKENHEIMER, A. LOIDL, C. R. OTTERMANN and K. BANGE, *Phys. Rev.* B **44**(11) (1991) 5927.
17. K. V. RAO and A. SMAKULA, *J. Appl. Phys.* **36**(6) (1965) 2031.
18. R. NEWMAN and R. M. CHRENKO, *Phys. Rev.* **114**(6) (1959) 1507.
19. SHIGEHARU KABASHIMA, *J. Phys. Soc. Japan.* **26**(4) (1969) 975.
20. M. A. KOLBER and R. K. MAC CORNE, *Phys. Rev. Lett.* **29**(21) (1972) 1457.
21. V. BIJU and M. ABDUL KHADAR, *Mater. Sci. Eng.* A **304–306** (2001) 814.
22. *Idem., Mater. Res. Bull.* **36** (2001) 21.
23. *Idem., J. Mater. Sci.* **36** (2001) 5779.
24. B. D. CULLITY, in "X-ray Diffraction," edited by Morris Cohen (Addison-Wesley Publishing Company Inc., 1959) p. 99.
25. R. J. MACDONALD, in "Impedance Spectroscopy: Emphasizing Solid Materials and Systems" (John Wiley and Sons, 1987) p. 12.
26. W. D. KINGERY, in "Introduction to Ceramics" (John Wiley and Sons, 1986).
27. A. K. JONSCHER, *J. Mater. Sci.* **13** (1978) 553.
28. M. SAYER, A. MANSINGH, J. B. WEBB and J. NOAD, *J. Phys. C. Solid. Stat. Phys.* **11** (1978) 315.
29. A. K. JONSCHER, *Philos. Mag.* B **38**(6) (1978) 587.
30. A. K. JONSCHER and J. M. REAU, *J. Mater. Sci.* **13** (1978) 563.
31. M. H. ABDULLAH and A. N. YUSOFF, *ibid.* **32** (1997) 5817.
32. B. PARVATHEESWARA RAO and K. H. RAO, *ibid.* **32** (1997) 6049.
33. M. SHAHIDI, J. B. HASTED and A. K. JONSCHER, *Nature* **258** (1975) 595.
34. R. BIRRINGER, *Mater. Sci. Eng.* A **117** (1989) 33.
35. C. SURYANARAYANA, *Bull. Mater. Sci.* **17** (1994) 307.
36. M. A. WITTENAUER and L. L. VAN ZANDT, *Philos. Mag.* B **46**(6) (1982) 659.
37. J. E. KEEM, J. M. HONIG and L. L. VAN ZANDT, *ibid.* **37**(4) (1978) 537.
38. C. M. OSBURN and R. W. VEST, *J. Phys. Chem. Solids.* **32** (1971) 1331.
39. C. M. OSBURN and R. W. VEST, *ibid.* **32** (1971) 1343.
40. THEODOROS KARAKASIDIS and MADELEINE MEYER, *Phys. Rev.* B **55**(20) (1997) 13853.

41. D. M. DUFFY and P. W. TASKER, *Philos. Mag.* A **50**(2) (1984) 193.
42. A. K. JONSCHER, *Nature* **250** (1974) 191.
43. *Idem.*, *ibid*. **253** (1975) 717.
44. *Idem.*, *ibid*. **256** (1975) 566.
45. *Idem.*, *ibid*. **267** (1977) 673.
46. K. L. NGAI, A. K. JONSCHER and C. T. WHITE, *Nature* **277** (1979) 185.
47. A. K. JONSCHER, *J. Mater. Sci*. **26** (1991) 1618.
48. *Idem.*, *J. Mater. Sci. Lett.* **17** (1998) 1975.
49. *Idem.*, *J. Phys. D. Appl. Phys*. **32** (1999) R57.
50. L. A. DISSADO and R. M. HILL, *Chem. Soc. Farady. Trans. 2*. **80** (1984) 291.

Received 23 October 2001
and accepted 7 July 2003